2011 IEEE International Conference on Robotics and Automation
Shanghai International Conference Center
May 9-13, 2011, Shanghai, China

Adaptive-Gain Complementary Filter of Inertial and Magnetic Data for Orientation Estimation

James Calusdian, Xiaoping Yun, and Eric Bachmann [1]

Abstract— **Accurate estimation of orientation based on data from small low-cost strapdown inertial and magnetic sensors is often inaccurate during highly dynamic motion or when trying to track movements that include two or more periods characterized by significantly different frequencies. This paper presents a complementary filtering algorithm for estimating orientation based on inertial/magnetic sensor measurements. The algorithm takes advantage of the complementary nature of the information offered by high-frequency angular rate sensor data and low-frequency accelerometers and magnetometers. The filtering algorithm utilizes a single gain that can be adaptively adjusted to achieve satisfactory performance while tracking two or more different types of motion. An additional feature of our approach involves the simple estimation of the gyro bias during periods exhibiting low dynamics and its subsequent use to correct the instantaneous gyro measurements. Simulation and experimental results are presented that demonstrate the performance of the algorithm during slow or nearly static movements, as well as, those which are highly dynamic. Experimental results indicate that the algorithm is able to track pitch and roll during dynamic motion with an RMS error of less than two degrees. This is believed to be superior to current proprietary commercial algorithms.**

Index Terms—**Accelerometers, inertial sensors, magnetic sensors, complementary filter, orientation estimation.**

I. Introduction

Orientation estimation based on the use of Micro Electro-Mechanical Systems (MEMS) sensors has resulted in applications in diverse areas, such as, cell phones, computer gaming, human posture tracking, robotics, and navigation [1][2][3]. Recently, commercial manufacturers have integrated MEMS accelerometers and gyros, along with magnetoresistive-type magnetometers, into a miniature strapdown inertial/magnetic measurement unit (IMMU). Applications involving these strapdown IMMUs can benefit from their small size, light weight, low power, and low cost. Additionally, orientation estimation derived from the IMMU has the advantage of utilizing measurements from naturally occurring references, such as the earth's magnetic field and gravity, and body angular rates of rotation. All of which do not require line-of-sight to some installed infrastructure which would lead to a limited range of use. Examples of commercially available IMMUs include the Intersense InertiaCube 2+ [4], the Xsens MTx [5], the Microstrain 3DM-GX3-25 [6], and the MEMSense nIMU [7]. Additionally, several of these manufactures currently produce an IMMU that incorporates embedded proprietary algorithms and are capable of three DOF (degree of freedom) orientation estimation.

However, orientation estimation accuracy is negatively impacted by physical limitations inherent in the MEMS accelerometers and gyros. These limitations manifest as noise present in the output of these sensors and can be quite large compared to that of navigation grade accelerometers and gyros resulting in undesirable attitude estimation error [8][9][10]. Calibration error arising from null-bias error, scale-factor error, and cross-axis coupling, which can be further influenced by the effects of aging and temperature, are also detrimental to the resulting attitude estimates [11].

Integration of the magnetometer into electronic systems results in sensor error that can also negatively affect the yaw angle estimate. Furthermore, these sensors are highly susceptible to interference from common everyday objects that can generate magnetic fields or influence the direction of the earth's magnetic field further affecting the desired attitude estimate [12].

Researchers have been attracted to the use of the IMMU for the obvious benefits, but have been challenged by the need to develop advanced and novel algorithms to mitigate the sensor errors. Algorithm development has evolved along two major paths. One approach incorporates the use of the ubiquitous Kalman filter while the other approach consists of the complementary filter. The former is attractive because it incorporates some knowledge of the noise statistics and when designed properly gives good results. The latter approach is attractive because it is straightforward and rather intuitive.

In [13], a solution is presented that incorporates, in a sense, two Kalman filters, which are adaptively selected based on whether the onset of accelerated motion has been detected. In [14] and also in [15], an extended Kalman filter is utilized. Here, as well, the filter is adaptively tuned in response to the measured acceleration.

The alternative approach found in the literature can be considered a frequency-based methodology in the form of the

[1] Manuscript received September 14, 2010. This work was supported in part by the National Science Foundation (NSF) and the Army Research Office (ARO).
James Calusdian is with the Department of Electrical and Computer Engineering, Naval Postgraduate School, Monterey, CA 93943 USA.
Xiaoping Yun is with the Department of Electrical and Computer Engineering and MOVES Institute, Naval Postgraduate School, Monterey, CA 93943 USA.
Eric R. Bachmann is with the Department of Computer Science and Software Engineering, Miami University, Oxford, OH 45056 USA.

complementary filter and has been presented in various sources including [16],[17],[18], and [19]. Our approach, as well, is based on the complementary filter, but incorporates a gain-switching strategy that is shown to give good results in a combination of low-dynamic and high-dynamic settings.

Generally speaking, attitude estimation can be classified into two main approaches. One involves the use of angular rate measurements obtained from orthogonally-mounted gyros. This in turn leads to the task of solving a set of differential equations involving either the direction cosine matrix or the attitude quaternion [20].

The alternative method for attitude estimation uses accelerometers and magnetometers to make measurements relative to gravity and the earth's magnetic flux density vector. Computation of attitude from these measurements is straightforward, as shown in [21] and [22].

This paper presents a simple complementary filter design that produces accurate three DOF estimates of orientation using MEMS accelerometers, magnetometers, and angular rate sensors. The filter is able to accurately track orientation during dynamic and slow movement. The filter algorithm utilizes a single gain, which is adaptively changed based on the type of movement to which the sensors are being subjected. Tracking accuracy is demonstrated through simulation studies and experiments involving a pendulum undergoing a variety of motion types. The intended application of the filter is tracking of foot orientation during stance and swing phases in a personal navigation system application [23]. However, the adaptive-gain design would be appropriate to other applications as well.

The remainder of this paper is organized as follows: Section II provides a description of the adaptive-gain complementary filtering algorithm. Section III describes a simulation study and results, which verify the operation of the filter and the response of the filter to noise. Experimental results obtained while using the filter to track the orientation of a real pendulum are described in Section IV. Section V reviews key findings of the paper and directions for future work.

II. Adaptive-Gain Quaternion-Based Complementary Filtering Algorithm

This section presents an adaptive-gain complementary filtering algorithm based on the use of inertial/magnetic sensor measurements. A block diagram of the complementary filter is shown in Figure 1. The complementary filter is designed to estimate the orientation of a rigid body, to which an IMMU is attached. The input to this filter are the nine components of the inertial/magnetic sensor measurements, which are three components of the accelerometer measurement $\vec{a}$, three components of the local magnetic field measurement $\vec{m}$, and three components of the angular rate measurement $\vec{\omega}$. The output of the filter is the estimated orientation represented by a quaternion $\hat{q}$. All measurements provided by the inertial/magnetic sensor module are relative to the sensor or body coordinate frame. To differentiate the same quantity in the body coordinate frame or the earth coordinate frame, a superscript is used to indicate the coordinate system. For example,

$$\vec{a}^{\,b} = \begin{bmatrix} a_x^b \\ a_y^b \\ a_z^b \end{bmatrix} \tag{1}$$

denotes the acceleration and its three components in the body coordinate frame.

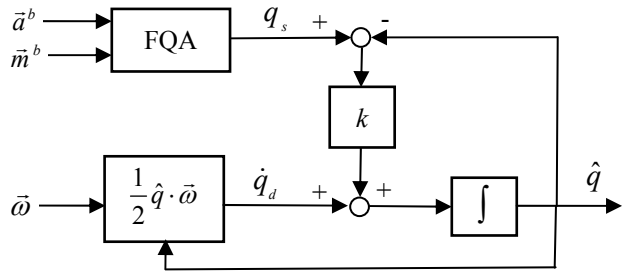

Figure 1. Block diagram of the adaptive-gain quaternion-based complementary filter of inertial and magnetic sensor measurements.

The orientation estimation filter is a type of algorithm that blends two sources of data in a complementary manner [24]. Specifically, the complementary filter shown in Figure 1 blends static information provided by the accelerometers and magnetometers, and dynamic information provided by the angular rate sensors. If the body to which the inertial/magnetic sensor module is attached is stationary or slowly moving, measurements provided by the accelerometer and magnetometer are sufficient to estimate the body orientation. However, if the body is subject to movement with relatively large linear acceleration, the orientation estimate based on the accelerometer and magnetometer measurements is no longer accurate. This is due to the fact that the accelerometer output is composed not only of the component of gravity measured along the sensor axis, but also the accelerated motion along this same axis. When in this dynamic state, the angular rate measurement is used for orientation estimation.

The complementary filter has two branches: the static quaternion branch q_s and the dynamic quaternion branch q_d. The static quaternion q_s is computed using the Factored Quaternion Algorithm (FQA) [25]. In the dynamic branch, a quaternion rate $\dot{q}_d$ is computed from the angular rate measurement $\vec{\omega}$ and the most recent quaternion estimate $\hat{q}$ using the well-known quaternion equation [26]:

$$\dot{q}_d = \frac{1}{2}\hat{q}\cdot\vec{\omega} \tag{2}$$

where the product between $\hat{q}$ and $\vec{\omega}$ is the quaternion multiplication and the angular rate $\vec{\omega}$ is cast into the form of a pure quaternion with the scalar part being equal to zero.

The FQA is a geometrically intuitive algorithm for determining orientation of a static or slow-moving body from measured acceleration and local magnetic field vectors. It is a

single-frame algorithm that takes measured acceleration and local magnetic field vectors at a given time and generates an orientation estimate without memory effect. The output orientation is represented by a quaternion. In this paper, the FQA is used in the static branch of the complementary filter to produce static quaternion q_s.

The filter gain k has the effect of adjusting the relative weight of the static and dynamic branches. The static quaternion q_s is compared with the most recent orientation estimate, $\hat{q}$, to produce a quaternion error $e(t) = q_s(t) - \hat{q}(t)$. The quaternion error $e(t)$ is multiplied by the feedback gain k, which is then used to correct the dynamic quaternion rate $\dot{q}_d(t)$. The corrected quaternion rate is then integrated to yield the estimated orientation in quaternion form. Though not shown in Figure 1, the estimated quaternion is immediately normalized to unit length.

The complementary nature of the orientation filter can be analyzed using the Laplace transform. Applying the principle of superposition and assuming that the input to the dynamic branch is zero, the transfer function from the static quaternion $Q_s(s) = \mathcal{L}\{q_s(t)\}$ to the estimated output quaternion $\hat{Q}(s) = \mathcal{L}\{\hat{q}(t)\}$ is given by:

$$H_s(s) = \frac{\hat{Q}(s)}{Q_s(s)} = \frac{k}{s+k}. \quad (3)$$

Now assuming that the input to the static branch is zero, the transfer function for the dynamic branch is given by:

$$H_d(s) = \frac{\hat{Q}(s)}{Q_d(s)} = \frac{s}{s+k}. \quad (4)$$

Equation (3) is a first-order low-pass filter with the corner frequency at $\omega_c = k$ and with a unit gain at very low or DC frequencies. On the other hand, equation (4) is a first-order high-pass filter with the same corner frequency $\omega_c = k$. Thus, at lower frequencies, the filter output relies more on the static quaternion $q_s(t)$ computed by FQA using the acceleration and local magnetic field measurements. At higher frequencies, the filter output relies more on the dynamic information provided by the angular rate measurements. At or near the corner frequency, the filter output is a fusion of both static and dynamic information. The corner frequency is determined by the choice of the feedback gain k. The optimal value for the filter gain depends on the application or motions, to which the sensor module is subjected. In general, if the sensor module is subjected to relatively slow motions, a larger filter gain is preferred. Conversely, if the sensor module is to experience relatively fast motions, a smaller filter gain is chosen.

The frequency response of the two branches of the complementary filter for three values of the filter gain $k = 0.01,\ 0.1,$ and 1.0 is shown in Figure 2. The response of the static branch shown in solid line is a low-pass filter, and the response of the dynamic branch shown in dashed line is a high-pass filter. The total output of the complementary filter is the sum of these two branches. It can be clearly seen that at lower frequencies the output of the complementary filter is dominated by the response of the static branch. At higher frequencies the total output is primarily contributed by the dynamic branch. At or near the corner frequency, the total output contains contributions from both branches. Depending upon the application in which the complementary filter is to be used, the filter gain can be optimized offline or adjusted in real time. For example, if the filter is used to estimate foot orientation during normal walking, foot motion alternates between a stance phase and a swing phase. During the stance phase, the foot is in a static or slow moving state and in the swing phase, the foot is in a dynamic state. Thus, it would be appropriate to use a large gain value while in the stance phase and a small gain value while in the swing phase when the foot is subject to fast movement. If the gain value is changed based on the gait phase, the filter can be expected to accurately estimate orientation through the entire gait cycle as documented in [27].

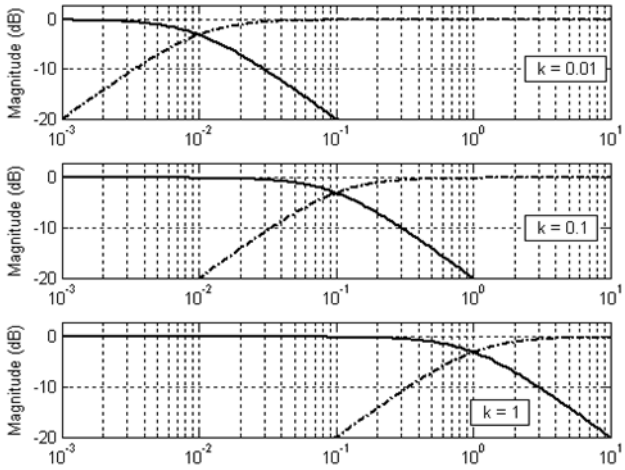

Figure 2. Magnitude Bode plot of the complementary filter with k=0.01, 0.1, and 1. The low-pass static branch is shown in solid line, and the high-pass dynamic branch is shown in dashed line

III. Simulation Results

The effectiveness of the complementary filter while changing the gain value based on dynamic state has been validated through simulation and physical experiments. In this section, simulation results are presented. Experimental results are described in the next section.

For simulation evaluation, a model of the vertical pendulum is introduced. The purpose of this model is to generate data to aid in the study of the performance of the complementary filter. In the model, an inertial/magnetic sensor module is attached at the swinging end of a pendulum. Theoretical expressions for the sensor data are derived that model the output of each sensor component when the pendulum was set into motion. In this manner, all of the real-world sensor artifacts, such as gyro bias, accelerometer offset, and motion-induced acceleration, which are understood to influence the orientation estimate, could be controlled and examined.

Figure 3 depicts a pendulum of length L. The angle of the pendulum is denoted by θ, with the positive rotation in the clockwise direction. An inertial/magnetic sensor module is considered to be attached to point A. A sensor or body

coordinate frame is shown in the figure, and is denoted by x^b–y^b–z^b. The inertial/magnetic sensor module is considered to have three orthogonally-mounted accelerometers, three orthogonally-mounted magnetometers, and three orthogonally-mounted angular rate sensors. When the accelerometers are subject to pendulum motion, in the absence of noise and misalignment errors, their outputs are characterized by [27]:

$$f_x = L\ddot{\theta} + g\sin\theta$$
$$f_y = 0$$
$$f_z = -L\dot{\theta}^2 - g\cos\theta$$

In the above equations, the values of θ, $\dot{\theta}$, and $\ddot{\theta}$ are obtained from simulated pendulum motion. As for the angular rate sensors, since the pendulum is constrained to swing in the x^b–z^b plane, only the angular rate sensor aligned with the y^b axis senses rotational motion. As such, the outputs of the three angular rate sensors are:

$$\omega_x = 0$$
$$\omega_y = \dot{\theta}$$
$$\omega_z = 0$$

The magnetometers measure the earth's magnetic flux density that is projected onto the sensor body axes. Assuming that the plane of the pendulum motion is aligned with magnetic north, the outputs of the magnetometers are given by:

$$m_x = \left|\vec{B}_e\right|\cos(\beta+\theta)$$
$$m_y = 0$$
$$m_z = \left|\vec{B}_e\right|\sin(\beta+\theta)$$

where the vector $\vec{B}_e$ is the earth magnetic flux density and β is the angle of inclination. The flux density vector and inclination angle vary over the time and from one location to another on the surface of the earth. In Monterey, CA, where the experiment was conducted, $\left|\vec{B}_e\right| = 0.486$ gauss and $\beta = 60.483$ degrees, which were obtained from the National Oceanic and Atmospheric Administration (NOAA) website.

The first simulation is designed to validate filter performance while using idealized sensors with no measurement noise. In particular, the angular rate sensors were assumed to be free of any noise or drift. In this case, with the filter gain $k = 0$, the filter is able to perfectly track the pendulum motion. Next, noise was introduced into the angular rate sensor measurement in the form of a small bias error. As expected with a filter gain $k = 0$, the estimated pitch angle tracked the true angle during the first few cycles, but began to drift away from the true track towards the end of the motion period. While the estimated roll and yaw angles were zero in the noiseless case, they now exhibited an error that grew without bound. The unbounded error with $k = 0$ is the result of relying solely on the integration of angular rate measurements.

Next, the value of k is gradually increased to determine the

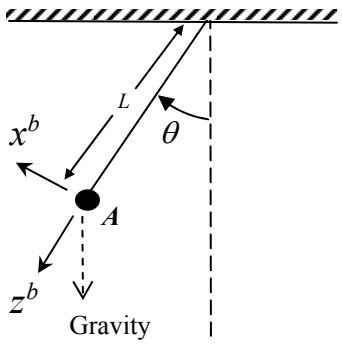

Figure 3. Schematic of the pendulum used in the simulation study.

effect of the FQA on the overall performance of the complementary filter. With the value of k on the order of 50, the unbounded error growth in the estimated roll and yaw angles is capped to a small constant error on the order of 0.002 degrees. However, the estimated pitch angle is unable to track the pendulum motion. This is due to the fact that accelerometers sense not only acceleration due to gravity, but also centripetal and tangential acceleration of the pendulum. With k set to a relatively high value, the complementary filter relies almost exclusively on accelerometer measurements processed by the FQA. This indicates that a gain value of 50 is too large.

The optimal value of k depends on motions of the pendulum. With a slow moving pendulum, a large value for k is more appropriate. Conversely, a smaller value for k is more appropriate for a fast-moving pendulum. Figure 4 shows the output of the complementary filter with $k = 1$. The estimation error in the pitch angle is less than one degree, and the error in the roll and yaw angles is about 0.1 degrees. The roll and yaw angle error is due to the presence of angular rate bias introduced into the measurement.

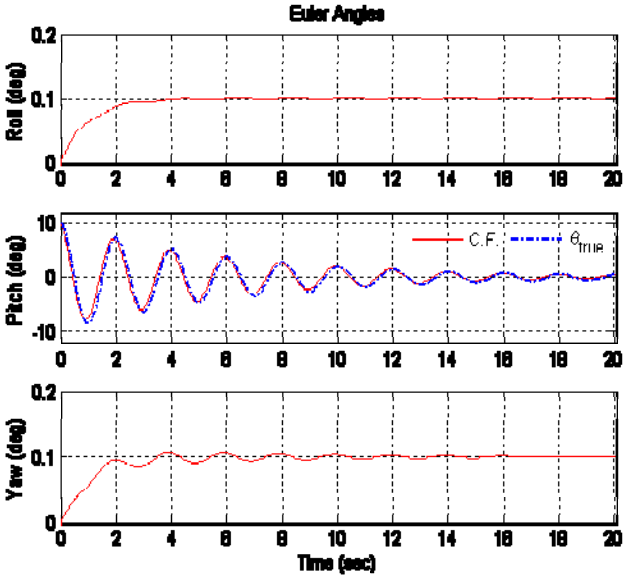

Figure 4. Complementary filter output (red) and the true pendulum angle (blue).

Extensive simulations validated the design concept and the complementary nature of the proposed filter. The performance of the filter can be optimized by adjusting the single filter gain. Further testing of the filter with real sensor data is described in the next section.

IV. Experimental Results

In this section, experimental results of the complementary filter using real sensor data are presented. To validate the performance of the complementary filter from real sensor data, an experimental apparatus shown in Figure 5 was constructed. It is a free-swinging pendulum with a MicroStrain 3DM-GX3-25 inertial/magnetic sensor module attached to the end. A 16-bit absolute optical encoder is positioned at the rotational axis to measure the pendulum motion. The readings from the encoder have an accuracy of 0.0055 degrees and are used as an angular reference. The apparatus is constructed of wood and placed on a wood tabletop to minimize magnetic interference. A LabView data acquisition program was developed for the National Instruments cRIO-9012 Real-Time Controller, which was an embedded computer that enabled more accurate program timing over a PC-based data acquisition system. The real-time controller read the raw counts from the 16-bit shaft encoder, as well as, the accelerometer, magnetometer, and gyro sensor data from the attached IMMU. All the data was arranged into a time-stamped array and written to a data file on the controller's hard drive. Later, the data file was imported into MATLAB for processing and analysis using our adaptive-gain complementary filter.

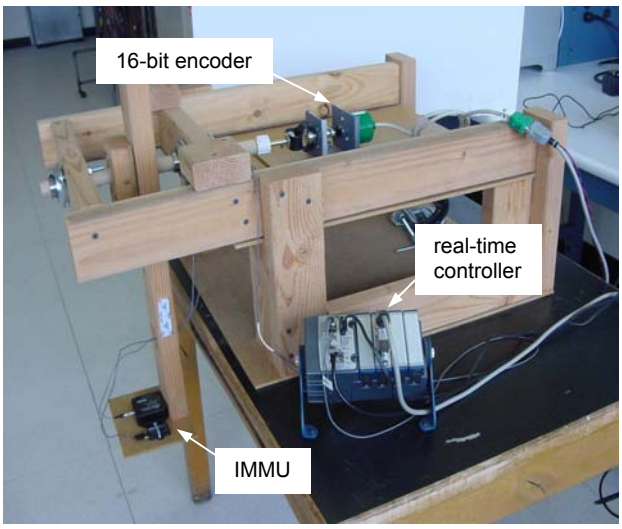

Figure 5. Pendulum apparatus constructed from wood materials to minimize the magnetic interference.

The complementary filter adaptively switched between two filter gain values during the experiment. For low dynamic motion, $k = 2.0$, and for high dynamic motion, $k = 0.00075$. These values were chosen experimentally to give satisfactory performance. Since the output of the complementary filter is a quaternion and not intuitively visualized, the result was converted into Euler angles. The corresponding roll, pitch, and yaw angles are plotted in Figure 6 for easy visualization.

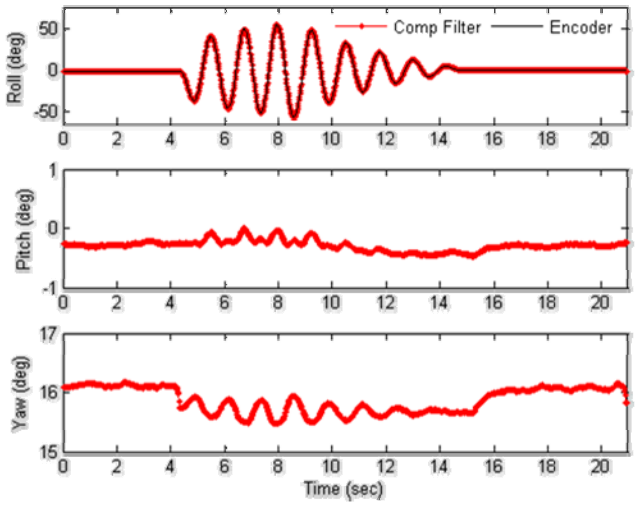

Figure 6. Estimated pendulum motion by the complementary filer in comparison with the reference provided by the encoder.

The sensor module is mounted at the end of the pendulum in such a way that the roll angle is aligned with the pendulum rotational axis. Figure 6 shows the roll, pitch, yaw angles of the pendulum when it is pushed back and forth manually (it is not swinging freely). The reference for the roll angle is provided by the encoder, whereas the reference for the pitch and yaw angles were taken to be those measured at the beginning of the experiment. It is seen that the estimated pitch and yaw angles are within 0.5 degrees of the assumed reference. It is not easy to see both the estimated roll angle and the reference roll angle as they are virtually on top of each other.

The difference between the estimated roll angle provided by the complementary filter and the reference roll angle provided by the encoder is shown in Figure 7. It is noted that the static error of the complementary filter (prior to the excited pendulum motion in the period of 0 to 4 seconds and after the excited motion in the period of 16 to 20 seconds) is virtually zero. The peak dynamic error is about 1.5 degrees. The root-mean-square (RMS) error of the estimated roll angle alone over the entire period is 0.35 degrees, and the RMS error for the estimated roll, pitch, and yaw angles is 0.49 degrees.

Figure 8 shows the result of another pendulum experiment where the pendulum is subjected to semi-random back-and-forth motion over a period of more than two minutes. Only the roll angle and its corresponding error is shown because the pitch and yaw angles are absent of significant motion as seen in Figure 6. In this case, the instantaneous error is more than 2.0 degrees in the time interval between 110 and 130 seconds. The overall RMS error of the estimated roll angle is 1.26 degrees. It is also noted that the static error returns to zero as soon as the pendulum stops moving in the time interval between 150 to 170 seconds, which is a result of switching the

k to a large value so that the filter uses weighs q_s more greatly in its output.

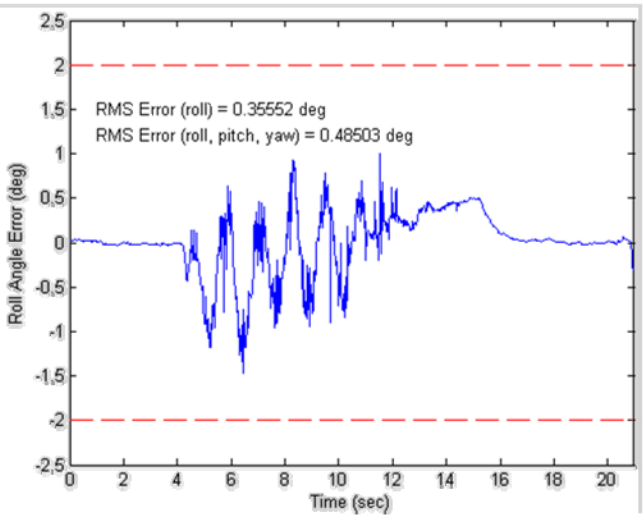

Figure 7. The error of the estimated roll angle shown in Figure 6.

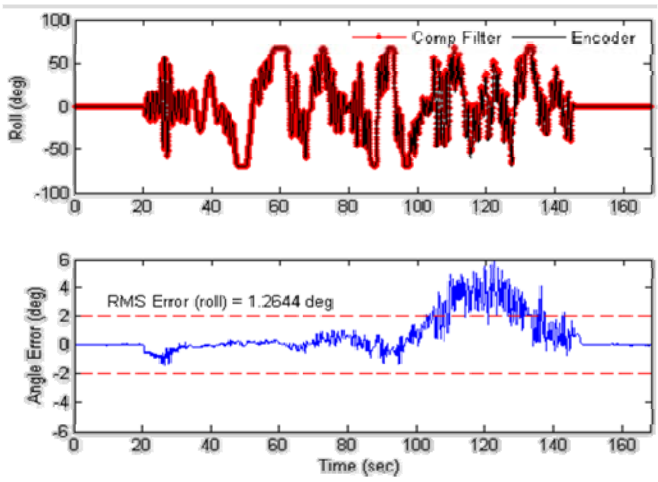

Figure 8. Estimated pendulum roll angle by the complementary filter versus the reference provided by the encoder (above) and the error of the roll angle (below).

In this and other experiments, the filter gain k is adaptively adjusted based on the magnitude of the angular motion indicated by the three-dimensional angular rate sensor measurement. While the filter gain could be continuously adjusted, a two-value switching strategy proved to be sufficient for the pendulum experiment. A lower k is used when the magnitude of the angular rate measurement is larger than a specified threshold, and a larger k is used otherwise.

Although not described in detail, an additional feature of our approach was the simple estimation of the gyro bias during periods exhibiting low dynamics. A first-order low pass filter estimated the bias based on the gyro measurements during the low-dynamic periods and was then used to correct the instantaneous gyro measurements provided to the complementary filter.

In summarizing the filter performance, it is noted that the dynamic accuracy of our adaptive-gain complementary filter is 0.485 degrees RMS for the first experiment and 1.264 degrees RMS for the second experiment. The static accuracy was not explored, but it is expected to be satisfactory as evidenced during the stationary periods of our experiments. Based on this, the dynamic performance of our approach is certainly comparable with that stated for the Microstrain 3DM-GX3-25. The manufacturer's stated orientation accuracy is 0.5 degrees under static conditions and 2 degrees under dynamic conditions using their undisclosed proprietary algorithm [6]. Our filter performance is also comparable with the dynamic accuracy stated for the Xsens MTx, which is 2 degrees RMS using their embedded sensor fusion algorithm [5]. We make a final comparison with [14], which described an approach based on the extended Kalman filter and demonstrated a noteworthy dynamic performance that was validated through actual experiment. The stated RMS error ranged from 4.57 to 9.01 degrees using the InterSense InertiaCube2, but subjected to a different type of motion testing. Arguably, the adaptive-gain complementary filter performs similarly with the additional benefit of requiring the adjustment of only one parameter to achieve satisfactory dynamic performance.

V. Conclusion

This paper presented the design and testing results of a quaternion-based complementary filter for estimating three-dimensional orientation from inertial/magnetic sensor data. The filter is simple and suitable for real-time implementation. It blends the high-frequency information provided by angular rate sensors and the low-frequency information provided by accelerometers and magnetometers. The effect of blending is accomplished by a single filter gain, whose value can be adaptively adjusted based on the motion to be estimated. The performance of the complementary filter with simulated and real pendulum motion data was presented. In particular, the dynamic performance and dynamic accuracy are documented. The RMS error of the estimated orientation is less than two degrees. The RMS error of the commercially available, low-cost MEMS inertial/magnetic sensor modules with proprietary algorithms is two degrees at the present time.

Acknowledgment

This work is in part supported by National Science Foundation under Agreement No. IIS-0964490, and Army Research Office.

References

[1] S. Beeby, G. Ensell, M. Kraft, and N. White, *MEMS Mechanical Sensors,* Artech House, Inc., Norwood, MA, 2004.
[2] H. Weinberg, "MEMS sensors are driving the automotive industry," *Sensors Magazine*, February 1, 2002.
[3] Tuite, D., "Motion-Sensing MEMS Gyros And Accelerometers Are Everywhere," Electronic Design, Vol. 57, No. 14, July 9, 2009.
[4] http://www.intersense.com/
[5] www.xsens.com

[6] www.microstrain.com
[7] www.memsense.com
[8] F. Mohd-Yasin, D. J. Nagel, C. E. Korman, "Noise in MEMS," *Measurement Science and Technology*, vol. 21, iss. 1, Article Number 012001, January 2010.
[9] T. B. Gabrielson, "Mechanical-thermal noise in micromachined acoustic and vibration sensors," *IEEE Transactions on Electron Devices*, vol. 40, no. 5, May 1993, pp. 903-909.
[10] R. P. Leland, "Mechanical-thermal noise in MEMS gyroscopes," *IEEE Sensors Journal*, vol. 5, no. 3, June 2005, pp. 493-500.
[11] D. Titterton and J. Weston, *Strapdown Inertial Navigation Technology, 2nd ed.*, The Institution of Electrical Engineers, Michael Faraday House, United Kingdom, and The American Institute of Aeronautics and Astronautics, USA, 2004.
[12] Microstrain, Inc., "3DM-GX1 hard iron calibration, ver. 3.1.00," September 19, 2005. [Online], Available: www.microstrain.com [Accessed: May 3, 2020].
[13] H. Rehbinder, X. Hu, "Drift-free attitude estimation for accelerated rigid bodies," *Robotics and Automation*, 2001. Proceedings 2001 ICRA, IEEE International Conference on, vol. 4, 2001, pp. 4244-4249.
[14] A. M. Sabatini, "Quaternion-based extended Kalman filter for determining orientation by inertial and magnetic sensing," *IEEE Transactions on Biomedical Engineering*, vol. 53, no. 7, July 2006, pp. 1346-1356.
[15] M. Wang, Y. Yang, R. R. Hatch, and Y. Zhang, "Adaptive filter for a miniature MEMS based attitude and heading reference system," *Position and Navigation Symposium*, April 26-29, 2004, pp. 193-200.
[16] R. Mahony, T. Hamel, J. M. Pflimlin, "Nonlinear complementary filters on the special orthogonal group," *IEEE Transactions on Automatic Control*, vol. 53, no. 5, June 2008, pp. 1203-1218.
[17] A. Tayebi, S. McGilvray, A. Roberts, and M. Moallem, "Attitude estimation and stabilization of a rigid body using low-cost sensors," *Proceedings of the 46th IEEE Conference on Decision and Control*, New Orleans, LA, USA, Dec. 12-14, 2007, pp. 6424-6429.
[18] A. El Hadri and A. Benallegue, "Attitude estimation with gyros-bias compensation using low-cost sensors," *Joint 48th IEEE Conference on Decision and Control and 28th Chinese Control Conference*, Shanghai, P. R. China, December 16-18, 2009, pp. 8077-8082.
[19] C. Dong, Q. Qiang, L. Chuntao, H. Chenglong, "Research of attitude estimation of UAV based on information fusion of complementary filter," *2009 Fourth International Conference on Computer Science and Convergence Information Technology*, pp. 1290-1293.
[20] R. McKern, H. Musoff, "Strapdown attitude algorithms from a geometric viewpoint," *Journal of Guidance, Control, and Dynamics*, 1981, vol. 4, no. 5, pp. 657-661.
[21] J. R. Wertz, *Spacecraft Attitude Determination and Control*, D. Reidel Publishing Company, Holland, 1978.
[22] M. D. Shuster, S. D. Oh, "Three-axis attitude determination from vector observations," *Journal of Guidance and Control*, vol. 4, no. 1. January-February 1981, pp. 70-77.
[23] X. Yun, E.R. Bachmann, H. Moore, and J. Calusdian, "Self-contained position tracking of human movement using small inertial/magnetic sensor modules," *Proceedings of IEEE International Conference in Robotics and Automation (ICRA), 2007*, Rome, Italy, May 2007, pp. 2526-2533.
[24] R. G. Brown and P. Y. C Hwang, *Introduction to Random Signals and Applied Kalman Filtering*, 3rd ed. New York, Wiley, 1996.
[25] X. Yun, E.R. Bachmann, and R.B. McGhee, "A simplified quaternion-based algorithm for orientation estimation from earth gravity and magnetic field measurements," *IEEE Transactions on Instrumentation and Measurement*, Vol. 57, No. 3, March 2008, pp. 638-650.
[26] J. B. Kuipers, *Quaternions and Rotation Sequences*. Princeton, NJ: Princeton Univ. Press, 1999.
[27] J. Calusdian, *A Personal Navigation System Based on Inertial and Magnetic Field Measurements*, Ph.D. dissertation, Naval Postgraduate School, Monterey, CA, September 2010.